AN ASSESSMENT OF THE FRACTURE TOUGHNESS ASSOCIATED WITH FLAT AND SLANT CRACK GROWTH IN A533B STEEL

I. S. Abou-Sayed, C. W. Marschall, and M. F. Kanninen

BATTELLE
Columbus Laboratories
Columbus, Ohio, USA

ABSTRACT

Experiments and finite element analyses were conducted to assess fracture toughness for flat ductile and slant (shear) fracture of ASTM A533 Gr. B steel. It was found that the differences are not large. Therefore, a resistance curve generated from flat fracture conditions can be used to predict stable crack growth and instability under slant or mixed slant and flat conditions.

KEYWORDS

Slant (Shear) Fracture, Flat Fracture, Fracture Toughness, A533B steel.

INTRODUCTION

Several investigators (Kanninen and co-workers, 1979, 1980; Shih and co-workers, 1979; Paris and co-workers, 1979; Hutchinson and Paris, 1979) have contributed to the development of a plastic fracture mechanics methodology to predict stable crack growth and instability in materials that exhibit strain hardening. One of the issues yet to be resolved in this work is the difference in fracture resistance (toughness) between flat ductile fracture and fractures that are partially or completely shear. This research was conducted to illuminate this problem. In the program, several A533B steel compact tension specimens were tested to obtain either flat ductile or shear fractures. A series of finite element analyses was performed to simulate these experiments in order to calculate different plastic fracture criteria (J, COD, COS, COA, etc) and assess the difference between the two types of fracture.

EXPERIMENTS

Compact tension specimens were machined from a 20 cm-thick plate of ASTM A533B steel which had previously been austenitized at 900 C, quenched, and tempered at 670 C. The composition and mechanical properties are shown in Table 1.

TABLE 1. Composition and Properties of A533B Steel Plate

Composition (percent by weight)

C	0.20	S	0.005
Mn	1.22	Si	0.15
P	0.011	Mo	0.55

Tensile Properties		Transition Temperature	
Yield Strength, MPa	520	Nil Ductility Transition (NDT)	-29C
Tensile Strength, MPa	650	Reference Temperature Nil Ductility Transition (RT_{NDT})	-29C
Elongation, pct in 50 mm	21		

The compact tension specimens used to investigate shear fracture contained a slant notch that terminated in a fatigue precrack. Figure 1 shows a slant-notch specimen after testing. The slant notch was used to promote single shear fracture from the very onset of crack extension; i.e., to avoid the transition from flat fracture to full shear that is observed with standard notch geometries. The specimens used to investigate flat ductile fracture contained side grooves to a depth of 12.5 percent on both front and back sides to hinder formation of shear lips. The test details are summarized in Table 2.

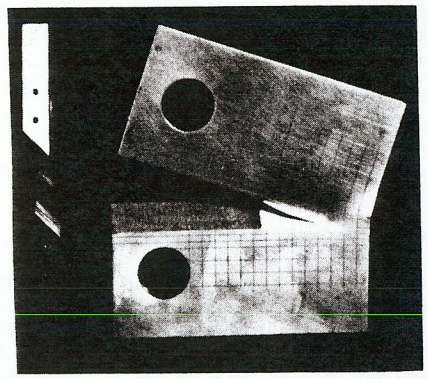

Fig. 1. Slant-notch specimen

As is evident in Fig. 1, the arms of slant notch specimens experienced out-of-plane displacement as the single-shear crack extended unless this was prevented by anti-buckling plates. The magnitude of this displacement was measured at the notch mouth at the completion of a test.

Data obtained from each specimen included load (P), load-line displacement (LLD), displacement at the original crack tip (COD), displacement at the current crack tip (crack opening stretch, COS), and the amount of crack growth (Δa).

The crack opening angle (COA) for a growing crack can be obtained from the slope, m, of a graph of COD versus Δa:

$$COA = 2\tan^{-1}(m/2) \quad .$$

TABLE 2. Summary of Experiments on A533B Steel

Specimen Number	Specimen Type	Fracture Type	Test Temp. C°	Width (W) mm (in)	Thickness (B) mm (in)	a_o/w
SR10.6	Slant-notch	Shear	24	177.8(7)	25.4(1)	0.4
SR10.7	Slant-notch	Shear	96	177.8(7)	25.4(1)	0.4
SR5.6	Slant-notch	Shear	20	101.6(4)	12.7(0.5)	0.4
SR5.9	Slant-notch	Shear	20	101.6(4)	12.7(0.5)	0.5
SR5.11	Slant-notch	Shear	20	101.5(4)	12.7(0.5)	0.6
SR2.6	Slant-notch	Shear	20	50.8(2)	6.35(0.25)	0.4
SR2.7	Slant-notch	Shear	20	50.8(2)	6.35(0.25)	0.4
SR1.6	Slant-notch	Shear	20	25.4(1)	3.18(0.125)	0.4
SR1.7	Slant-notch	Shear	20	25.4(1)	3.18(0.125)	0.4
SR1.6A[(a)]	Slant-notch	Shear	20	101.6(4)	3.18(0.125)	0.4
1S	Side-grooved	Flat	93	50.8(2)	25.4(1)	0.5
2S	Side-grooved	Flat	93	50.8(2)	25.4(1)	0.5

(a) Anti-buckling plates were used because of large w/B ratio.

Figure 2 shows results for shear crack extension in specimens of different sizes. It can be seen that, although the COD at initiation is independent of specimen size, the COA (as indicated by the slope, m) diminishes as the specimen size increases. Figure 3 summarizes the influence of specimen dimensions on the COA for shear fracture extension. Note that both specimen thickness (B) and the ratio of width (W)-to-thickness play a role.

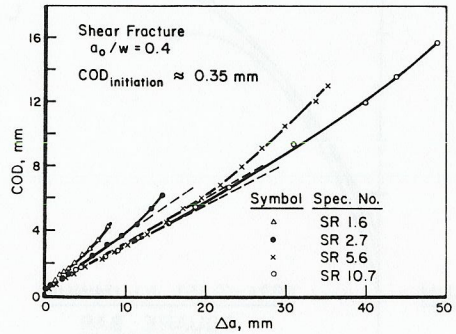

Fig. 2. COD versus Δa for slant fracture in slant notch specimens

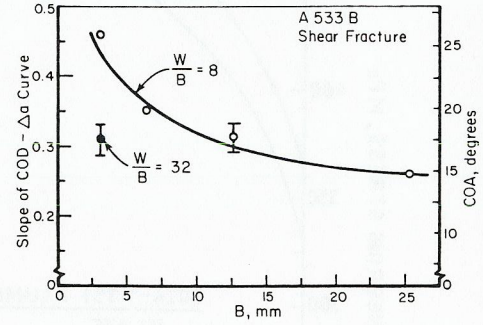

Fig. 3. Effect of specimen dimensions on COA

A similar effect of specimen dimensions on the COA was observed for flat fracture extension. However, only two specimen sizes were examined; one in this study and one in a companion study conducted by Shih and co-workers (1979) on the same heat of A533B steel. Shih's results yielded COA values of 8 to 10 degrees for 4T compact tension (CT) specimens, whereas values of 15 to 16 degrees were found for IT-CT specimens in this program. In both studies, the initiation-COD values for flat ductile fracture were not well defined but appeared to bracket the value of about 0.35 mm found for shear fracture.

The displacement measured at the advancing crack tip (COS) was also examined for

its ability to characterize stable crack growth. Figure 4 shows COS versus Δa for slant-notch specimens of several sizes. The COS value is seen to increase at a diminishing rate as the crack extends, finally reaching a plateau, the level of which is dependent on specimen dimensions. The findings of the COS studies for shear fracture are summarized in Fig. 5. It can be seen that both B and the W/B ratio influence the plateau values of COS.

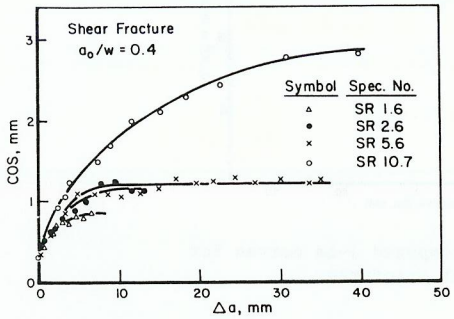

Fig. 4. COS versus Δa for slant fracture in slant notch specimens

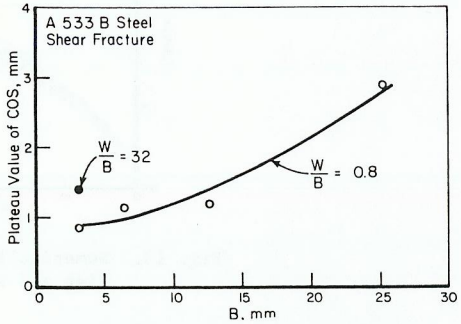

Fig. 5. Effect of specimen dimensions on plateau value of COD

A limited study of COS for flat ductile fracture yielded similar results; i.e., large specimens exhibited greater plateau values of COS than did small specimens. Tests conducted by Shih and co-workers (1979) on 4T-CT specimens showed plateau values of COS to be about 1.1 to 1.4 mm, whereas tests on 1T-CT specimens in this program gave values of 0.6 to 0.8 mm.

If, as is often assumed, both COA and COS are indicators of propagating-crack toughness, the two parameters yield contradictory results relative to specimen size effects. COA values indicate that increasing the specimen size decreases the toughness, whereas COS values indicate the opposite effect. This observation suggests that neither the COA nor the COS is a suitable parameter for characterizing the stable crack propagation resistance for A533B steel, either for shear or for flat ductile fracture, under plane stress conditions.

The data obtained in the crack growth experiments permit yet another characterizing parameter to be computed: the J-integral. These values were calculated by the method of Garwood, Robinson, and Turner (1975) from records of P, LLD, and Δa. It should be noted that values of J at initiation were relatively imprecise because the test techniques did not clearly define the onset of crack extension. J-resistance curves are presented in Fig. 6 for different specimen sizes and fracture types. The curves suggest that: (1) J-values for shear fracture are not strongly influenced by specimen dimensions, and (2) J-values for flat, ductile fracture do not differ appreciably from those for full shear fracture for the A533B steel tested here.

FINITE ELEMENT ANALYSIS

Generation phase finite element analyses were carried out for a more detailed study of the flat and slant-fracture experiments. Four specimens were analyzed: three slant-fracture specimens (Battelle specimens SR2.6, SR5.6, and SR10.7) and one flat-fracture specimen (General Electric Company specimen T52, as reported by Shih and co-workers, 1979). In these analyses, the finite element model was forced to reproduce an experimentally measured applied load (or load line displacement) versus crack growth record. While the crack is growing by releasing crack tip nodes, various crack tip parameters, including J-integral, COA, crack-tip opening angle (CTOA), are computed from the model.

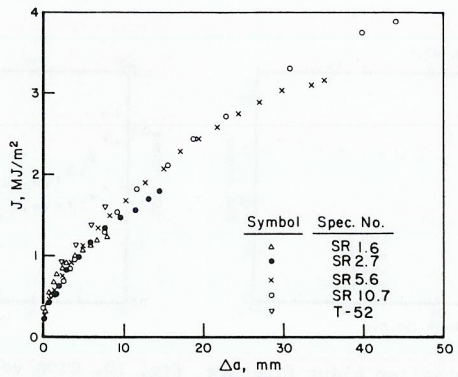

Fig. 6. J-Δa curves for flat and slant fractures

Two-dimensional finite element grids were constructed to represent the mid plane of each specimen. The slant-fracture specimens were analyzed under plane stress conditions, while the flat-fracture specimen was analyzed with plane strain conditions. Figure 7 shows the experimental LLD versus Δa record used as input to the analysis of slant-notch specimen SR5.6. The accuracy of the finite element model in simulating the actual experiment can be determined by comparing the predicted P-LLD curve with the experimentally measured curve. The comparison for experiment SR5.6 is shown in Fig. 8. This good agreement is typical of all the other specimens analyzed.

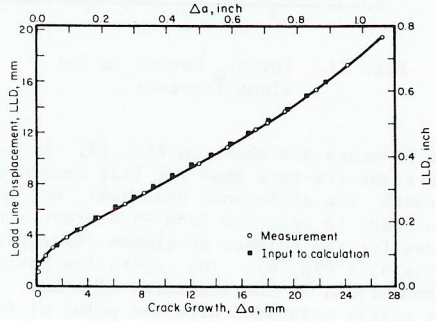

Fig. 7. LLD versus Δa for slant notch specimen SR 5.6

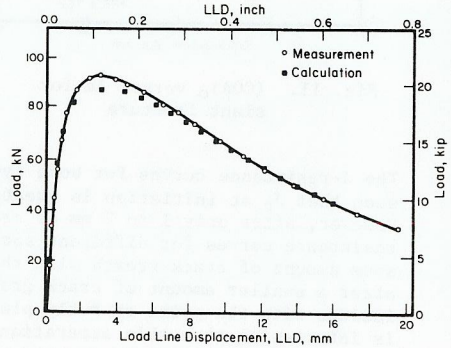

Fig. 8. P versus LLD for slant notch specimen SR 5.6

RESULTS AND DISCUSSION

Figures 9 and 10 show the COA and CTOA resistance curves for all analyzed specimens representing both flat and shear fractures. It can be seen that while COA is specimen thickness dependent (see also Figure 3), CTOA is thickness independent after the initial transient part. These comparisons show an apparent difference between flat and slant fractures. However, if a factor of $\sqrt{2}$ is introduced to define a consistent angle which is included in a plane perpendicular to the fracture surfaces, then the difference between flat and slant fractures becomes almost nonexistent. This is shown in Figs. 11 and 12.

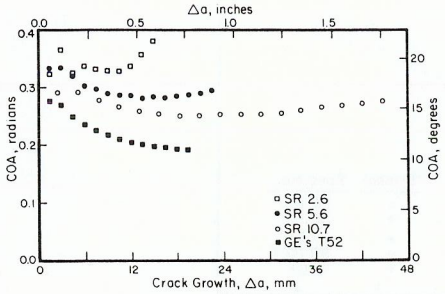

Fig. 9. COA versus Δa for slant fracture

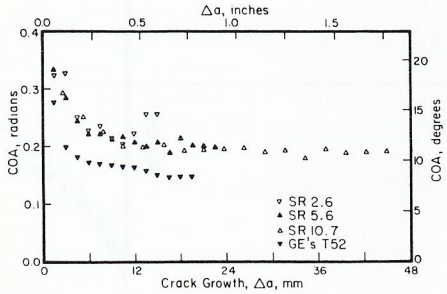

Fig. 10. CTOA versus Δa for slant fracture

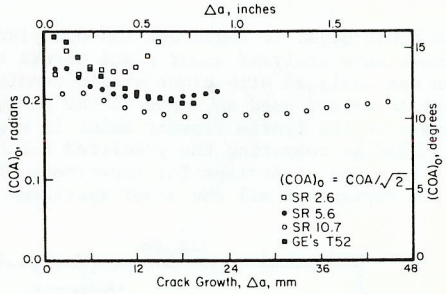

Fig. 11. $(COA)_o$ versus Δa for slant fracture

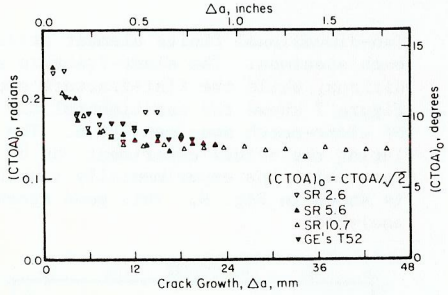

Fig. 12. $(CTOA)_o$ versus Δa for slant fracture

The J-resistance curves for both types of fracture are shown in Fig. 13. It is seen that J_c at initiation is greater for slant fracture than for flat fracture. However, after only 1 to 2 mm of crack growth, the difference vanishes. But the J-resistance curves for different specimens start to separate from each other after some amount of crack growth with the curves for the thinner specimens diverging after a smaller amount of crack growth (see also Fig. 6). The separation point coincides with the point of fully plastic conditions in the remaining ligament. It is interesting that this separation point nearly coincides with the point of inflection on the LLD versus Δa experimental records (Kanninen and co-workers, 1980). This behavior of the J-resistance curve in the fully plastic condition indicates that a slight specimen size dependence exists. Similar results were also reported by Rice and co-workers (1979). However, it is important to recognize that the CTOA resistance curve does not show this dependence.

CONCLUSIONS

Experimental and analytical results show that the growing-crack toughness of A533B steel, as characterized by J-resistance, COA, and CTOA, does not differ much between flat ductile and slant modes of fracture. It was found also that, under fully plastic conditions, the J-resistance curve shows a slight specimen size dependence. Such a dependence is not observed in the CTOA resistance curve. This suggests that the CTOA approach has an advantage in predicting extended amounts of crack growth under fully plastic conditions.

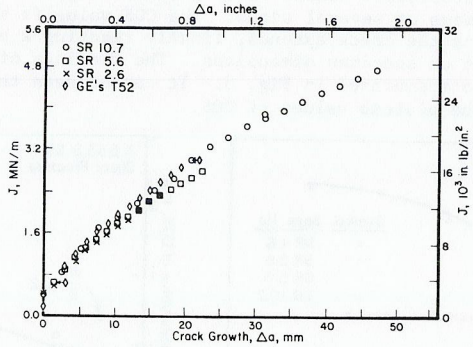

Fig. 13. Numerically computed J-Δa curves for flat and slant fractures

ACKNOWLEDGEMENT

This work was supported by the Electric Power Research Institute under RP601-1. Dr. T. U. Marston was the project manager. The authors acknowledge the valuable contributions made to this study by their colleagues at Battelle, Dr. D. Broek, Dr. G. T. Hahn, and Mr. R. B. Stonesifer.

REFERENCES

Garwood, S. J., J. N. Robinson, and C. E. Turner (1975). The measurement of crack growth resistance curves (R. curves) using the J-integral. International Journal of Fracture, 11, 528-532.

Hutchinson, J. W., and P. C. Paris (1979). Stability analysis of J-controlled crack growth. In J. D. Landes, J. A. Begley, and G. A. Clarke (Eds.), Elastic-Plastic Fracture, ASTM STP 668, American Society for Testing and Materials, 37-64.

Kanninen, M. F., E. F. Rybicki, R. B. Stonesifer, D. Broek, A. R. Rosenfield, C. W. Marschall, and G. T. Hahn (1979). Elastic-plastic fracture mechanics for two dimensional stable crack growth and instability problems. In J. D. Landes, J. A. Begley and G. A. Clarke (Eds.), Elastic-Plastic Fracture, ASTM STP 668, American Society for Testing and Materials, 121-150.

Kanninen, M. F., G. T. Hahn, D. Broek, R. B. Stonesifer, C. W. Marschall, I. S. Abou-Sayed, and A. Zahoor (1980). Methodology for plastic fracture - phase II. Battelle's Columbus Laboratories, Final Report to EPRI on RP601-1.

Paris, P. C., H. Tada, A. Zahoor, and H. Ernest (1979). The theory of instability of the tearing mode of elastic-plastic crack growth. In J. D. Landes, J. A. Begley and G. A. Clarke (Eks.) Elastic-Plastic Fracture, ASTM STP 668, American Society for Testing and Materials, 5-36.

Rice, J. R., W. J. Drugan, and T. L. Sham (1979). Elastic plastic analysis of growing cracks. Brown University Technical Report No. COO-3084/65. Providence, R.I. Also to appear in ASTM-STP.

Shih, C. F., H. G. deLorenzi and W. R. Andrews (1979). Studies on crack initiation and stable crack growth. In J. D. Landes, J. A. Begley, and G. A. Clarke (Eds.), Elastic-Plastic Fracture, ASTM STP 668, American Society for Testing and Materials, 65-120.